

# **SHEAR BEHAVIOR OF ANCHORAGES WITH STANDOFF INSTALLATION**

## **QUERZUGVERHALTEN VON BEFESTIGUNGEN MIT ABSTANDSMONTAGE**

Baran Deniz Upcin, Michael Yamandu Eckstein, Vinay Mahadik, Jan Hofmann  
*Institute of Construction Materials (IWB), University of Stuttgart*

### **SUMMARY**

This paper investigates the shear behaviour of anchors in stand-off installation within the analytical framework of EN 1992-4, based on Scheer's plastic-limit concept. A parametric finite element analysis is conducted using ANSYS. The investigated parameters include lever arm length, degree of fixture rotational restraint, embedment depth, anchor diameter, and the presence or absence of nut bearing against the concrete surface. The anchor's shear resistance and the internal load transfer mechanism are evaluated. The bending moment demand is evaluated with reference to the plastic limit value. The aim is to provide a concise, mechanics based basis for assessing the anchor's shear resistance in stand-off installation in accordance with EN 1992-4.

### **ZUSAMMENFASSUNG**

Diese Arbeit untersucht das Scherverhalten von Ankern bei Abstandsmontage im analytischen Rahmen von EN 1992-4 auf der Grundlage des plastischen Grenzkonzepts nach Scheer. Eine parametrische Finite-Elemente-Analyse wird mit ANSYS durchgeführt. Die untersuchten Parameter umfassen die Hebellarmlänge, den Grad der rotationalen Einspannung der Befestigung, die Verankerungstiefe, den Ankerdurchmesser sowie das Vorhandensein oder Fehlen einer Mutterauflage auf der Betonoberfläche. Der Querkraftwiderstand des Ankers und der innere Lastübertragungsmechanismus werden bewertet. Das erforderliche Biegemoment wird im Hinblick auf den plastischen Grenzwert ermittelt. Ziel ist es, eine prägnante, mechanikbasierte Grundlage für die Beurteilung des Querkraftwiderstands von Ankern bei Abstandsmontage gemäß EN 1992-4 bereitzustellen.

## 1. INTRODUCTION

Design approaches for anchors have matured into codified methods, notably EN 1992-4 [1]. Stand-off installations are common in practice; the offset between the attachment and the concrete surface creates a lever arm, so the anchor shank is subjected to combined shear and bending. While the code framework addresses these effects in a simplified manner, important aspects are not sufficiently characterized; most notably, the distribution of load transfer across the embedment under loading.

Laboratory testing provides the primary evidence, but it is costly, slow, and difficult to scale across multiple diameters, embedments, and boundary conditions. Variability in concrete and geometric tolerances complicates comparisons. In contrast, high-fidelity finite element analysis (FEA) offers an efficient and complementary approach. Nonlinear models can implement controlled boundary conditions, capture contact and local bearing, and provide repeatable parametric scans.

In this study, a parametric FEA is performed in ANSYS® [2] to examine stand-off shear under pure shear loading. The focus is on the steel response and on the associated load transfer in the concrete. Results are read against design expressions and assumptions from current standards and prior research, without going into detail here.

### 1.1 Design framework and reference equations

In order to investigate the influence of anchorage depth and lever arm on the shear force and bending moment resistance of anchors with stand-off installation, the assumptions of Eurocode 1992-4 [1] and the research conducted by Scheer (1987) [3] on the bending moment capacity of screw anchors were taken as references.

In cases without a lever arm, the characteristic steel shear resistance of the anchor is defined in EN 1992-4 [1] as

$$V_{Rk,s}^0 = k_6 A_s f_{uk} \quad (1)$$

where  $A_s$  denotes the steel area and  $f_{uk}$  the characteristic ultimate tensile strength of the steel. The coefficient  $k_6$  is taken as 0.6 for  $f_{uk} \leq 500 \text{ N/mm}^2$  and as 0.5 for  $500 < f_{uk} \leq 1000 \text{ N/mm}^2$ . This expression represents the reference resistance in the absence of a lever arm and serves as the basis for assessing the reduction in capacity caused by bending.

In stand-off installations, the anchor is subjected to a bending moment, and the shear resistance is expressed as

$$V_{Rk,s} = \frac{(\alpha_M M_{Rk,s})}{l_a} \tag{2}$$

with the lever arm  $l_a = e_1 + a_3$ . The restraint factor is  $\alpha_M = 1.0$  (Figure 1a) for free rotation and  $\alpha_M = 2.0$  (Figure 1b) for full restraint.

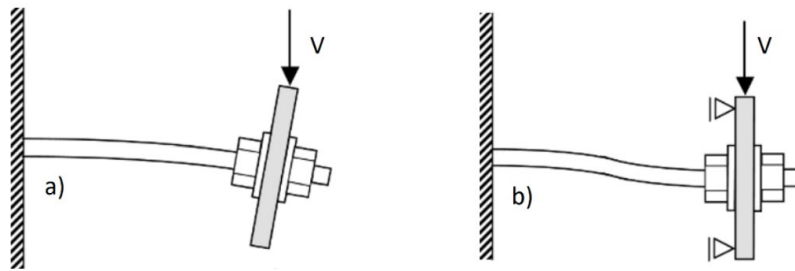


*Fig. 1: Anchor installation without (a) and with (b) fixture restraint [1]*

The geometric term reflects the contact condition at the concrete surface, where nut bearing is present with  $a_3 = 0$  and nut bearing is absent with  $a_3 = 0.5 d_{nom}$  (as shown in Figure 2)

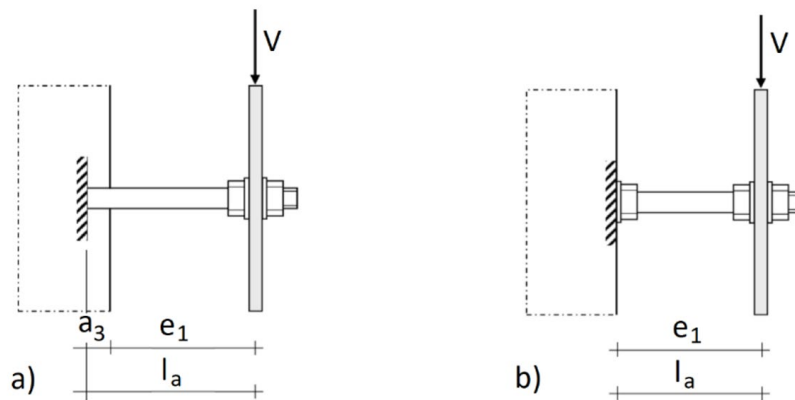


*Fig. 2: Lever arm definition for bending verification; a) without nut bearing, b) with nut bearing [1]*

Since this study considers only pure shear, the axial force is taken as  $N_{Ed} = 0$  and the interaction between bending and tension reduces to  $M_{Rk,s} = M_{Rk,s}^0$ . Here

$M_{Rk,s}^0$  denotes the characteristic bending capacity of the steel element as provided by product data or established mechanical estimates.

Scheer's [3] plastic-limit moment is used as a reference for the bending demand in stand-off shear. The characteristic plastic moment is taken as

$$M_{pl,k} = 0.90 W_{pl} f_{uk} \quad (3)$$

Here,  $f_{uk}$  is the characteristic ultimate tensile strength of the steel, and  $W_{pl}$  is the plastic section modulus at the critical section. For round sections, the plastic modulus may be approximated by

$$W_{pl} = 1.7 \frac{\pi}{32} d^3 \quad (4)$$

The diameter  $d$  is the shank diameter if bending localizes in the smooth shank, or the thread root (stress) diameter if localization occurs in the threaded zone.

The simulation results were evaluated against the EN 1992-4 [1] formulations and Scheer's [3] plastic-limit moment and were interpreted within these two reference frameworks.

## 2. DETAILS OF THE PARAMETRIC STUDY

A parametric finite-element study was carried out in ANSYS to examine stand-off shear under pure shear loading. Only the steel failure mechanism and the associated load transfer in concrete were considered; edge breakout, pry-out, group effects, and cyclic actions were excluded. All geometric dimensions were parameterized by the nominal anchor diameter  $\emptyset$  to enable non-dimensional interpretation. Concrete properties corresponded to class C20/25; steel properties were consistent with common construction grades (yield strength = 500 MPa).

As shown in Figure 3, four boundary-condition configurations were considered. The notation combines nut bearing on the concrete surface (first symbol) and fixture rotational restraint (second symbol): 0-0 (no bearing; rotation free), 0-X (no bearing; rotation restrained), X-0 (bearing present; rotation free), and X-X (bearing present; rotation restrained). These configurations were used throughout the matrix.

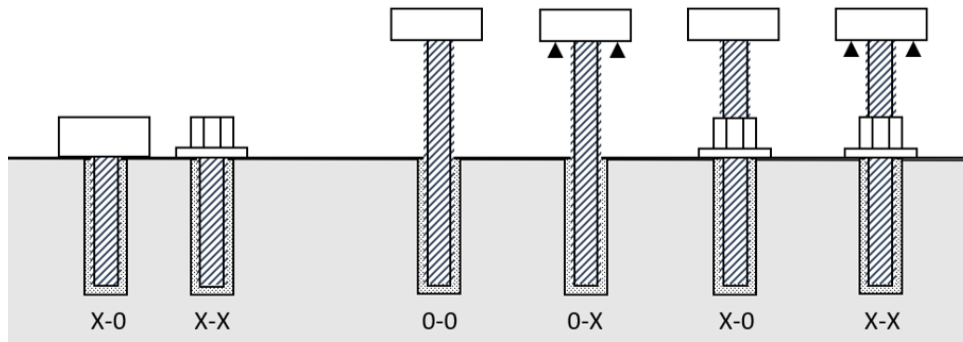


Fig. 3: Boundary-condition configurations investigated in the parametric study

The parameter matrix covered three anchor diameters (M6, M12, M20) and three embedment depths ( $h_{ef} = 5\varnothing, 10\varnothing, 15\varnothing$ ); at each embedment, the lever arm  $Z$  took the values  $\varnothing, 0.5h_{ef}, 1.0h_{ef}$ , and  $1.5h_{ef}$ . The combinations used are summarized in Table 1.

Table 1: Lever arm ( $Z$ ) as a function of embedment depth ( $h_{ef}$ )

DIAMETER	$\varnothing$		
EMBEDMENT DEPTH	$5 \varnothing$	$10 \varnothing$	$15 \varnothing$
LEVER ARM	$\varnothing$	$\varnothing$	$\varnothing$
	$0.5 \times 5 \varnothing$	$0.5 \times 10 \varnothing$	$0.5 \times 15 \varnothing$
	$1.0 \times 5 \varnothing$	$1.0 \times 10 \varnothing$	$1.0 \times 15 \varnothing$
	$1.5 \times 5 \varnothing$	$1.5 \times 10 \varnothing$	$1.5 \times 15 \varnothing$

In total, 126 simulations were run to cover all combinations of diameter, embedment, lever arm, and boundary condition configuration.

### 3. RESULTS & DISCUSSION

Following Scheer [3], two failure criteria were adopted for evaluating the simulations. For ductile failure, the limit load  $V$  is defined at a global rotation of  $10^\circ$ . If the load–rotation curve reaches its peak before  $10^\circ$ , the behaviour is classified as non-ductile failure, and  $V$  is taken as the maximum attained load. All results were interpreted with these criteria to enable a consistent comparison across failure types.

### 3.1 Effect of lever arm and restraint on shear resistance

In Figures 4, 5, and 6 of this study, the simulated steel shear capacities for 6, 12, and 20 mm anchors are plotted against the lever arm to diameter ratio. In all cases, the capacity decreases steeply as the lever arm increases, reflecting the growing bending demand on the anchor shank.

Boundary conditions have a pronounced influence. The fully restrained, nut-bearing configuration (X-X) consistently attains the highest capacities, whereas the fully unrestrained case without nut and with free rotation (0-0) yields the lowest. The intermediate configurations (X-0 and 0-X) lie between these extremes and are relatively close to each other.

In Figures 4, 5, and 6, the dashed line represents the Eurocode [1] steel shear resistance without a lever arm. Agreement is good for very small lever arms, but the discrepancy increases rapidly as the lever arm grows.

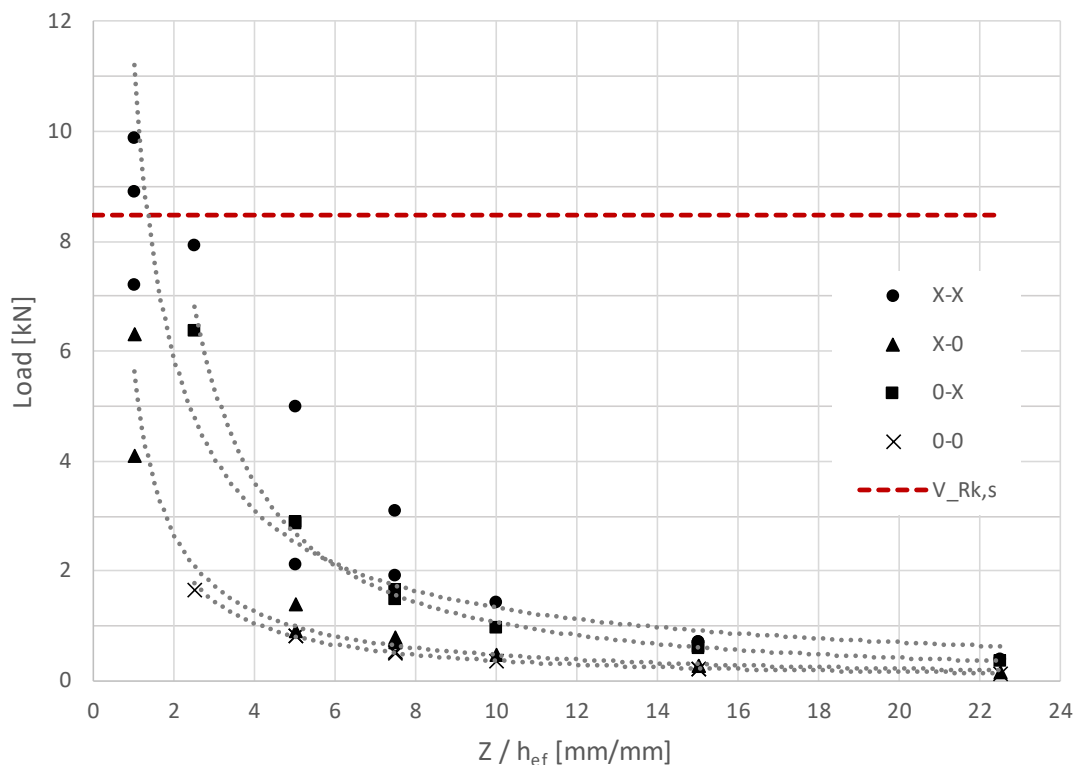


Fig. 4: Shear resistance of Ø6 anchors vs. lever arm ratio  $Z/h_{ef}$

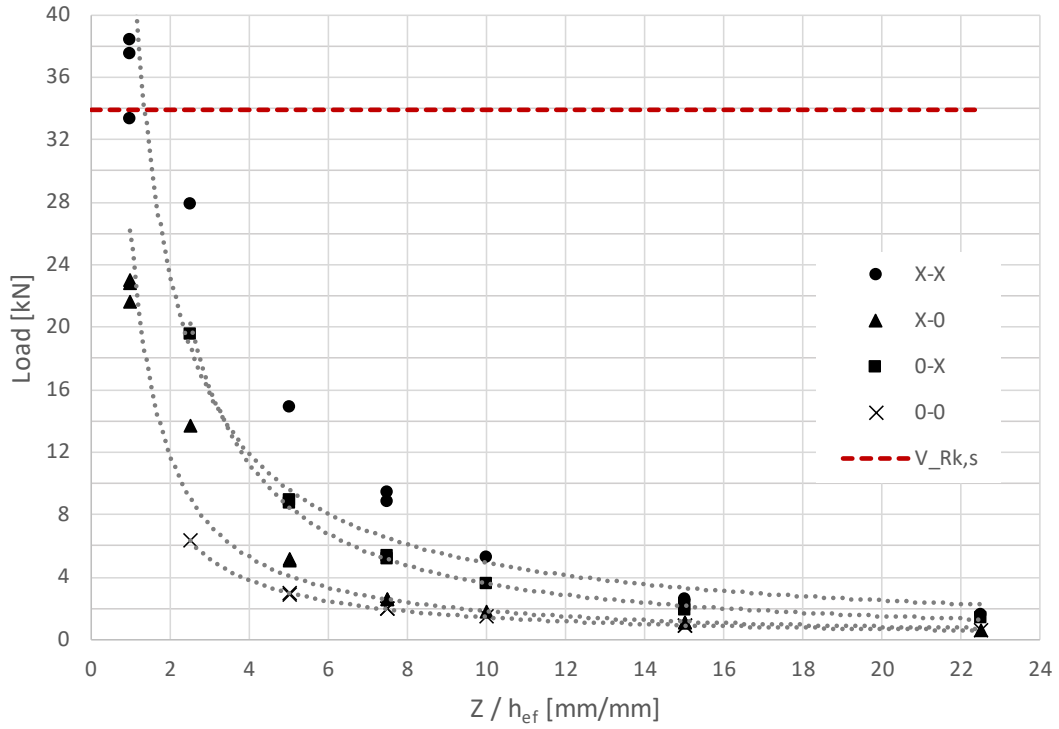


Fig. 5: Shear resistance of Ø12 anchors vs. lever arm ratio  $Z/h_{ef}$

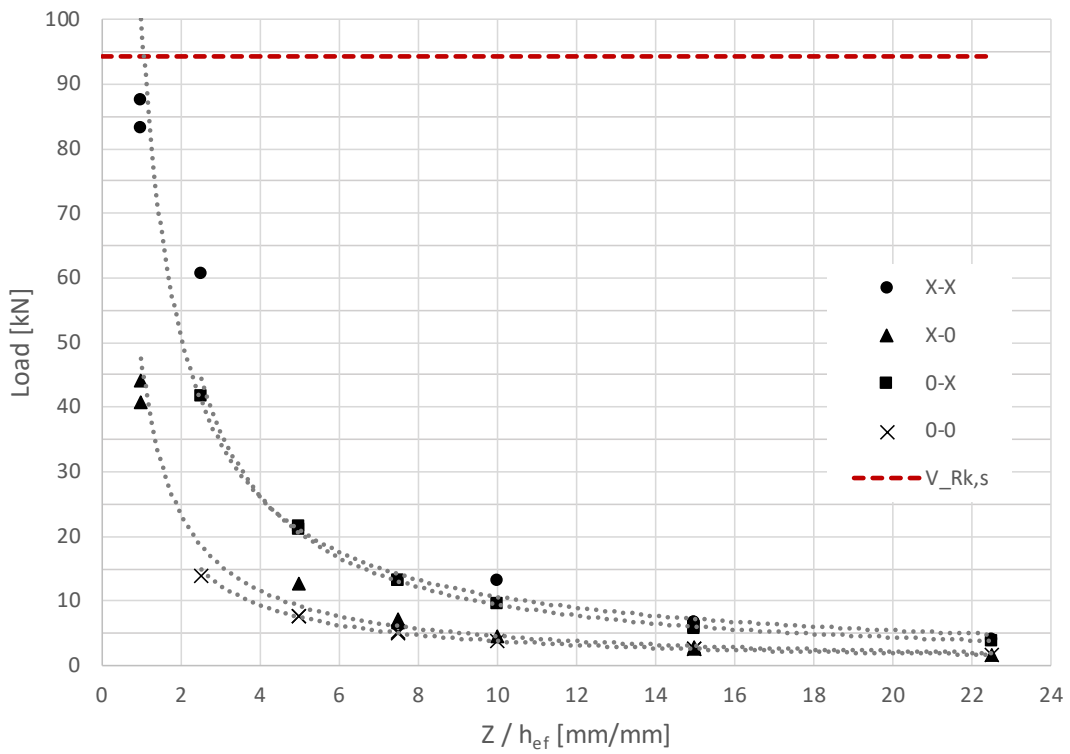


Fig. 6: Shear resistance of Ø20 anchors vs. lever arm ratio  $Z/h_{ef}$

### 3.2 Evaluation of bending moment and comparison with Scheer

In this chapter, two boundary conditions were distinguished for extracting bending moments from the FE results. The first condition corresponds to the case without nut bearing (0-0, 0-X), as shown in Figure 7(a). In this configuration, the external shear force  $F$  acting at the lever arm  $Z$  induces a bending field within the embedment. The first non-zero concrete contact reaction, denoted as  $R_1$ , occurs at a depth  $X_1$  below the concrete surface. A second resultant  $R_2$  may develop deeper in the embedment at distance  $X_2$ . Based on a hand calculation using the FE force resultants, it becomes evident that the maximum bending moment occurs at the critical section located at  $X_1$ . This section corresponds to the onset of concrete bearing and coincides with the peak curvature zone in the free rotation case.

The second condition occurs when the fixture is clamped by a nut and washer, which restrains rotation and shifts the maximum bending moment to the concrete surface, as shown in Figure 7(b). In practice, the critical section is taken directly at the concrete surface just below the nut or washer, since the geometric discontinuity combined with the restraint produces the largest curvature at this location. Accordingly, the hand calculated bending moment is evaluated at  $X=0$ .

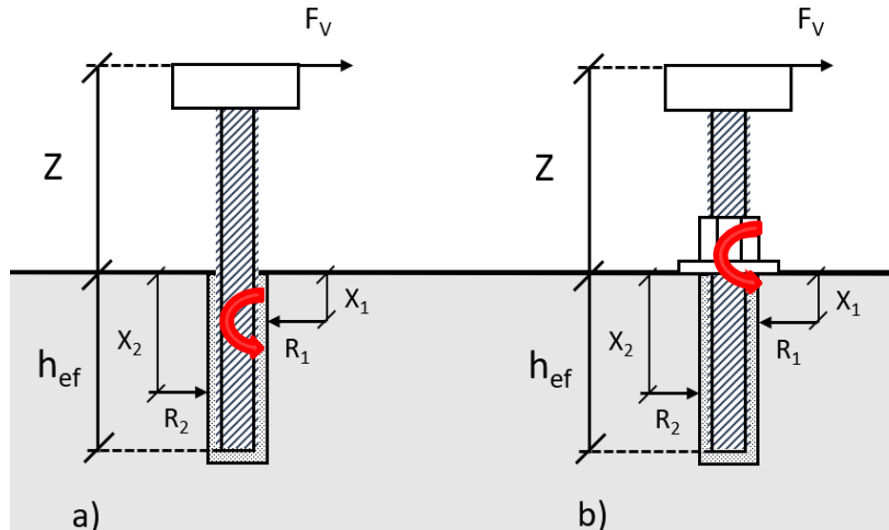


Fig. 7: Resisting moment with and without nut bearing on the concrete surface

In Figures 8 and 9, the bending moments obtained from the FE results are compared with the plastic limit moment  $M_{k,sp}$  proposed by Scheer [3]. For clarity, the moments are normalized by  $M_{k,sp}$ , and the lever arm is given relative to the anchor diameter ( $Z/\varnothing$ ) to avoid size effects. The dashed line in the graphs shows where ANSYS ® results equal Scheer's [3] plastic limit ( $M/M_{k,sp}=1$ ).

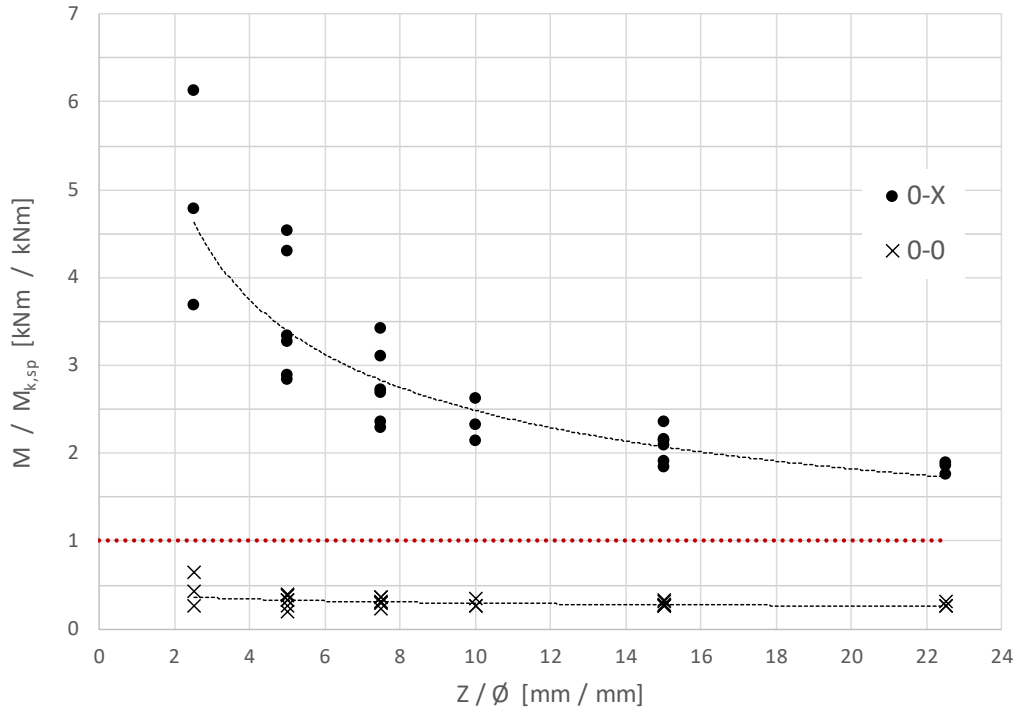


Fig. 8: Normalized bending moment vs. lever arm ratio for anchors without nut bearing on the concrete surface (configurations 0-X and 0-0)

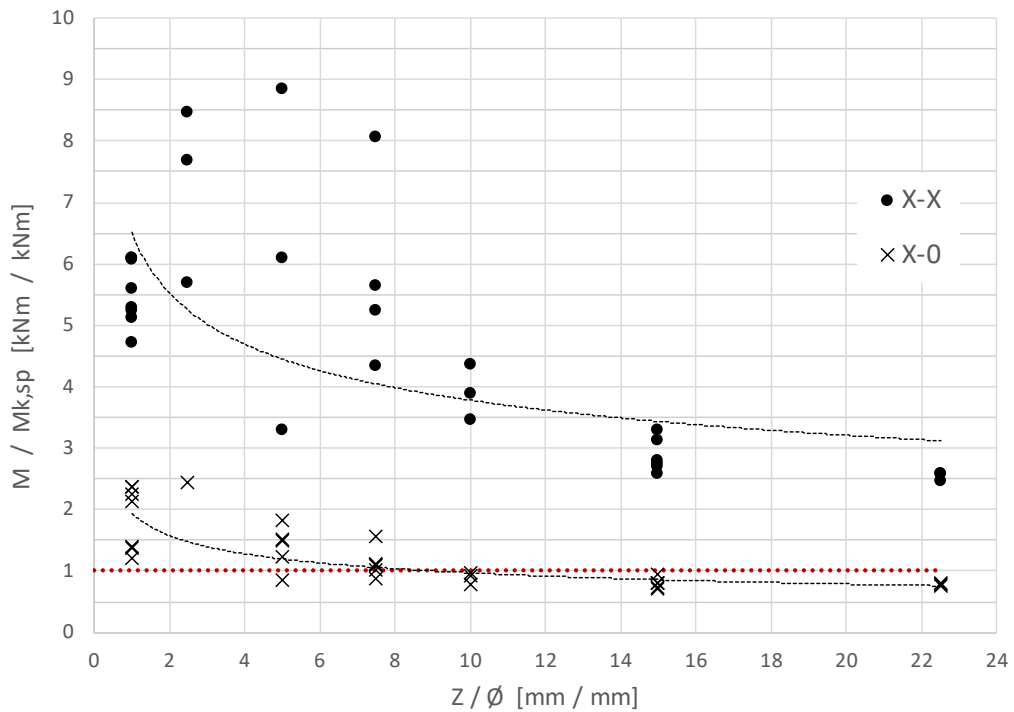


Fig. 9: Normalized bending moment vs. lever arm ratio for anchors with nut bearing on the concrete surface (configurations X-X and X-0)

Without nut bearing (0-0), the normalized moments stay well below one, usually between 0.3 and 0.7, showing that free rotation strongly reduces the mobilized moment. When rotation is restrained, the values are much higher. In the case without nut bearing but with restraint (0-X), the normalized moments range from about 2 to 6, depending on the lever arm length. When the nut clamps the fixture against the concrete surface (X-X), the maximum moment ratio, reaching values between 5 and 9 for short lever arms and decreasing to about 3 to 4 for longer ones. The semi-restrained case (X-0) also exceeds the plastic limit, but to a smaller degree, with values typically between 1.0 and 2.5.

### 3.3 Effective rotational restraint factor $\alpha_M$

To isolate the influence of the rotational restraint factor, pairs of FE models were selected that differed only in the degree of fixture restraint, while all other parameters such as geometry, embedment depth, nut presence, and material properties were kept constant. According to EN 1992-4 [1], when these parameters remain unchanged, the ratio of shear resistances between the restrained and unrestrained cases is determined solely by  $\alpha_M$ . Accordingly, the effective  $\alpha_M$  was obtained directly from the FE results as  $\alpha_M = V_r / V_u$ , where  $V_r$  (restrained) and  $V_u$  (unrestrained) are the characteristic shear capacities of two otherwise identical models. Two sets of ratios were evaluated: X-X / X-0 for nut-bearing configurations and 0-X / 0-0 for stand-off configurations without nut bearing.

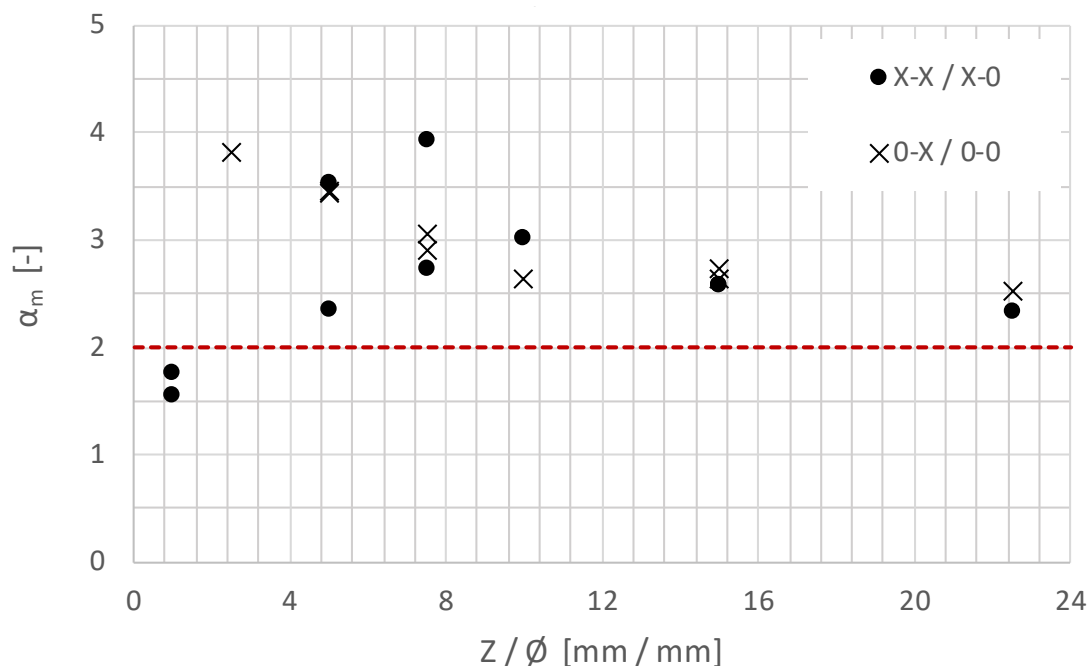


Fig. 10: Effective rotational restraint factor  $\alpha_M$  for  $\varnothing 6$  anchors vs.  $Z/\varnothing$

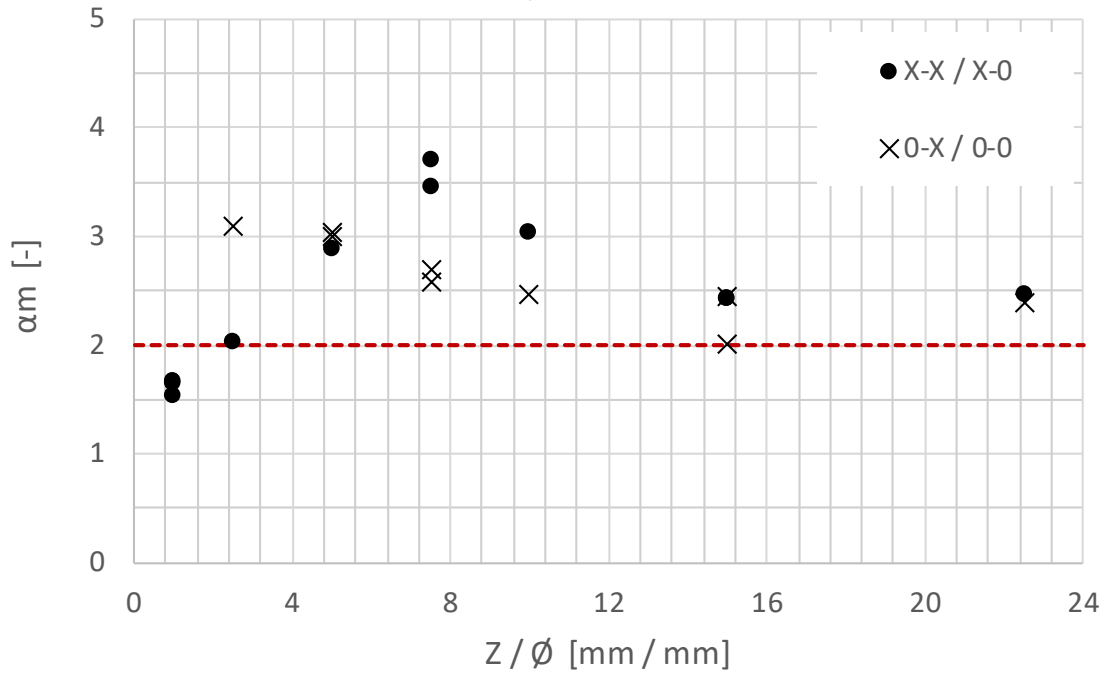


Fig. 11: Effective rotational restraint factor  $\alpha_M$  for  $\varnothing 12$  anchors vs.  $Z/\varnothing$

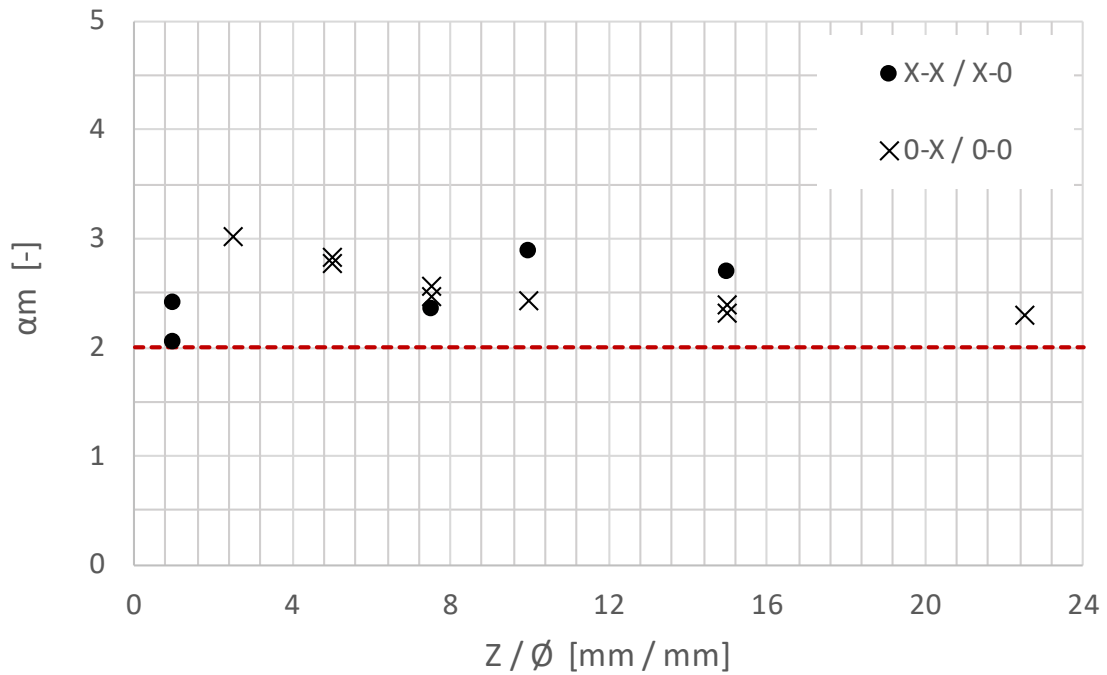


Fig. 12: Effective rotational restraint factor  $\alpha_M$  for  $\varnothing 20$  anchors vs.  $Z/\varnothing$

In Figures 10, 11, and 12, the rotational restraint factor  $\alpha_M$  varies with the normalized lever arm for different anchor diameters. In principle, EN 1992-4 [1]

prescribes  $\alpha_M = 1.0$  for free rotation and  $\alpha_M = 2.0$  for full restraint, but the FE simulations reveal a more nuanced response.

For small diameters ( $\emptyset 6$ ,  $\emptyset 12$ ), the effective  $\alpha_M$  often exceeds 2.0, reaching about 3–4 at short lever arms. This suggests that nut clamping and fixture stiffness provide stronger rotational restraint in slender anchors. For larger diameters ( $\emptyset 20$ ), the simulated  $\alpha_M$  values cluster near 2.0, indicating that the Eurocode simplification is reasonably accurate for stockier anchors.

### 3.4 Validation of the eurocode eccentricity $a_3$ using FE results

As noted in Section 1.1, EN 1992-4 [1] introduces an additional eccentricity term  $a_3$  that depends on whether the nut and washer bear directly on the concrete surface. In stand-off configurations,  $a_3 = 0$  when direct bearing is present; when nut bearing is absent,  $a_3 = 0.5 \times d_{nom}$ , and the lever arm is taken as  $l_a = e_1 + a_3$ . The FE simulations provide a physical interpretation of this definition: in cases without nut bearing, the maximum bending moment does not occur at the concrete surface but at a depth  $X_1$  where the first significant concrete reaction develops (see the previous section). In this section, the proximity of  $X_1/\emptyset$  to 0.5 is assessed using the plots below, and the Eurocode assumption is discussed.

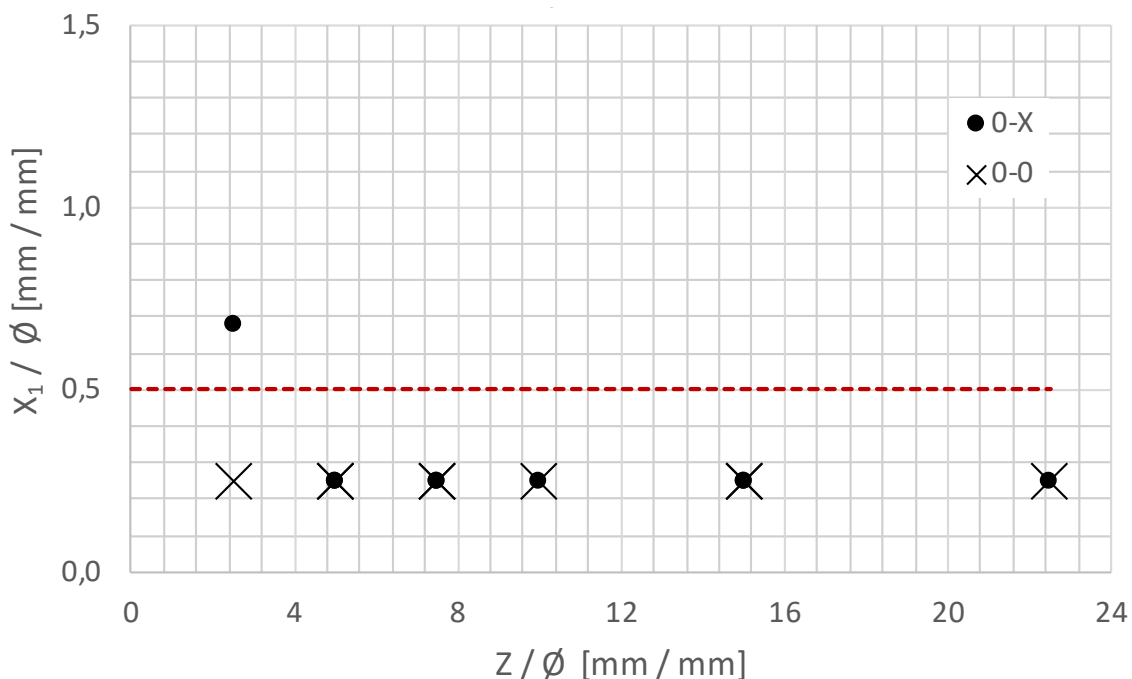


Fig. 13:  $X_1 / \emptyset$  for  $\emptyset 6$  anchors compared to Eurocode assumption ( $a_3 = 0.5 \times d_{nom}$ )

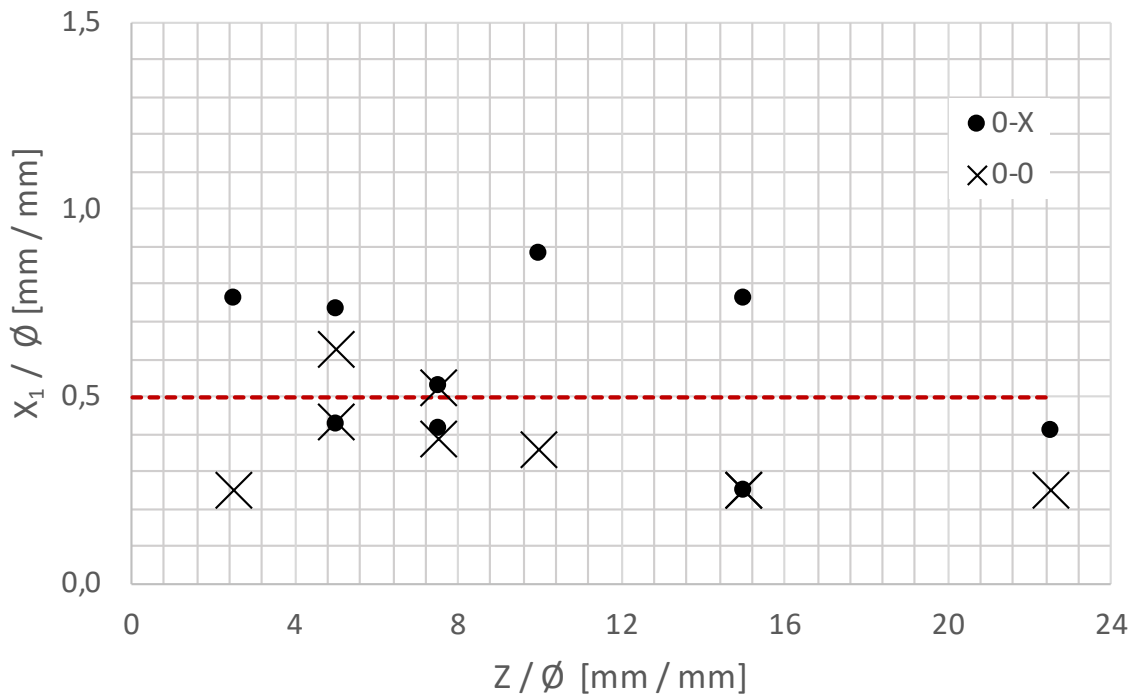


Fig. 14:  $X_1 / \varnothing$  for  $\varnothing 12$  anchors compared to Eurocode assumption ( $a_3 = 0.5 \times d_{nom}$ )

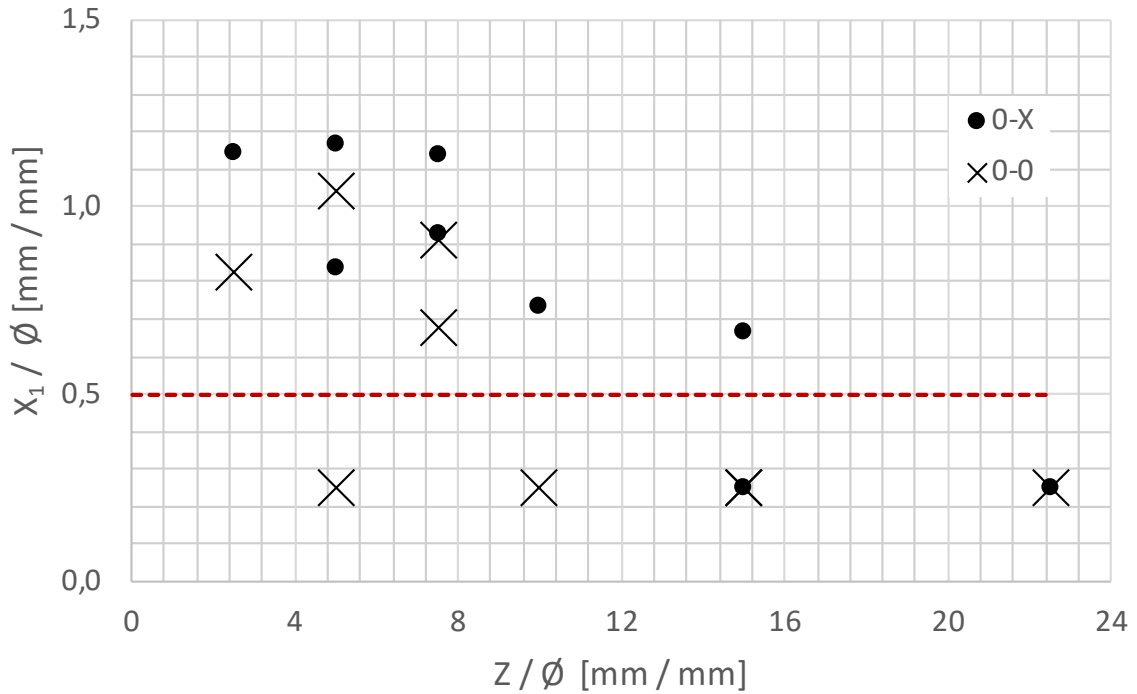


Fig. 15:  $X_1 / \varnothing$  for  $\varnothing 20$  anchors compared to Eurocode assumption ( $a_3 = 0.5 \times d_{nom}$ )

In Figures 13, 14, and 15, the ratio  $X_1/\emptyset$  is plotted against the lever arm ratio  $Z/\emptyset$ . The dashed line marks the Eurocode [1] reference  $a_3/\emptyset = 0.5$ . The results show no consistent dependence on the lever arm; instead, the depth ratio is mainly governed by anchor diameter and rotational restraint, with 0-X generally deeper than 0-0. For  $\emptyset 6$ , most values cluster around  $X_1/\emptyset \approx 0.25$  clearly below 0.5. For  $\emptyset 12$ , the results are scattered around 0.5 (about 0.4–0.6). For  $\emptyset 20$ , the spread is widest (0.25 to 1.2), and many restrained points lie above 0.5.

Overall,  $X_1/\emptyset$  tends to be below 0.5 for small diameters, near 0.5 for medium diameters, and above 0.5 for large diameters. This indicates a clear diameter effect and suggests that the fixed assumption  $a_3 = 0.5 \times d_{nom}$  may not represent all cases well. It overestimates the effective depth for small anchors and underestimates it for large anchors.

### 3.5 Effective embedment zone

This last section examines how the depths of the concrete bearing resultants vary with the lever arm in stand-off shear. The first resultant depth  $X_1$  (location of the initial concrete compression resultant) and the second resultant depth  $X_2$  (deeper compression resultant that develops as loading progresses) are evaluated for each simulation. To remove diameter effects and enable comparison across sizes, both quantities are plotted in normalized form as  $X_1/h_{ef}$  (in Figure 16) and  $X_2/h_{ef}$  (in Figure 17). The horizontal axis is the lever arm ratio  $Z/h_{ef}$ . The dataset includes all four boundary-condition configurations used throughout the study, so that the influence of nut bearing and rotational restraint on the load-transfer depths can be assessed jointly with the lever arm.

For the first resultant depth  $X_1/h_{ef}$ , values are scattered and relatively high at small lever arm ratios  $Z/h_{ef}$ . As  $Z/h_{ef}$  increases,  $X_1/h_{ef}$  decreases rapidly and stabilizes within a narrow band of about 0.02–0.10 for  $Z/h_{ef} \approx 1.0$ –1.5. Rotational restraint (X-X, 0-X) pushes the resultant deeper; free rotation (X-0, 0-0) keeps it shallower.

For the second resultant depth  $X_2/h_{ef}$ , the spread is wide at small  $Z/h_{ef}$  ( $\approx 0.2$ –0.8). With increasing lever arm, the values contract and settle in the 0.20–0.60 band. The same pattern holds: restraint places the resultant deeper, whereas free rotation concentrates in the lower part of the band. Nut bearing has a secondary influence compared with rotational restraint.



## 4. CONCLUSIONS

Based on the results of the parametric study, it can be concluded that the main trends are clear: steel shear resistance falls rapidly as the lever arm increases. This behaviour is consistent across diameters and embedment depths and reflects the growing bending demand in the shank. Rotational restraint at the fixture has a strong effect: restrained configurations reach higher resistances and larger moments than free cases. An effective restraint factor can be inferred from capacity ratios, but it depends on geometry and boundary conditions; it is not a universal constant.

Scheer's [3] plastic-limit moment provides a useful benchmark. Finite-element moments stay below this limit for freely rotating fixtures, while clamped cases with small lever arms can approach or exceed it. The Eurocode [1] eccentricity  $a_3$  gains a physical meaning through the FE-observed depth  $x_1$  of the first concrete resultant. The fixed value  $a_3=0.5 \times d_{\text{nom}}$  captures the order of magnitude but does not represent all diameters and restraints equally well.

These findings provide a compact, mechanics-based basis for assessing the shear resistance of anchors in stand-off installation within the EN 1992-4 [1] framework. The study is limited to pure shear and single anchors, and does not cover concrete breakout, pry-out, group effects, or cyclic loading. Future work should include validation tests, a quantitative measure of fixture stiffness for restraint, studies on combined shear–tension loading, and refined code parameters for the concrete-surface eccentricity component of the lever arm and for rotational restraint.

## REFERENCES

- [1] DIN EN 1992-4:2018: *Eurocode 2 – Design of concrete structures – Part 4: Design of fastenings for use in concrete*; German version EN 1992-4:2018. DIN Deutsches Institut für Normung e.V., Berlin, 2018
- [2] ANSYS®, 2022 R2: Ansys® Academic Student, Release 2022 R2, 2022
- [3] SCHEER, J.: *Schrauben mit planmäßiger Biegebeanspruchung*. Bericht Nr. 6079, Institut für Stahlbau der Technischen Universität Braunschweig, Braunschweig, 1987